Comparative Evaluation of Magnetic Activated Carbon Synthesised Using Chemical Co-Precipitation and Impregnation for Heavy Metal Removal

[1]Abdulmalik Musa, [2]Badruddeen S. Sani, [3]Umar A. Abubakar, and [4]Donatus B. Adie
[1]Department of Chemical Engineering, Nasarawa State University, Keffi, Nigeria
[1,2,3,4] Department of Water Resources and Environmental Engineering, Ahmadu Bello University, Zaria, Nigeria
musaabdulmalik@nsuk.edu.ng|bssaulawa@abu.edu.ng|uaabubakar@abu.edu.ng|donadie2005@yahoo.com

Received: 24-MAY-2026; Reviewed: 09-JULY-2026; Accepted: 18-JULY-2026
https://dx.doi.org/10.46792/fuoyejet.v11i3.1596

ORIGINAL RESEARCH

Abstract— Magnetic activated carbons (MACs) have demonstrated potential for the elimination of heavy metal because of their adsorption efficiency and ease of post-treatment recovery. However, limited research has systematically evaluated how different magnetisation routes influence physicochemical properties, adsorption performance, and production cost for wastewater treatment systems. This study synthesised and comparatively evaluated MACs produced via chemical co-precipitation (CP-MAC) and chemical impregnation (CI-MAC) using activated carbon as precursor. Characterisation was conducted using textural analysis, morphology, elemental composition, functional groups, point of zero charge (pH_{PZC}), and bulk density. Experiments involving batch adsorption techniques were performed using chromium as the model heavy metal, and equilibrium analysis of the data was conducted through nonlinear models based on Langmuir and Freundlich theories. CP-MAC exhibited a pH_{PZC} of 5.30 compared to 7.90 for CI-MAC and 8.20 for pristine AC. CP-MAC achieved a maximum monolayer adsorption capacity (q_m) of 9.40 mg/g, exceeding CI-MAC (6.03 mg/g). Langmuir model provided superior fit, with R^2 values of 0.98 (RMSE = 0.30) and 0.95 (RMSE = 0.40) for CP-MAC and CI-MAC respectively. Economic evaluation revealed lower unit production cost for CP-MAC (₦127/g) compared to CI-MAC (₦146/g). The results demonstrate that chemical precipitation method offers better performance under the conditions studied.

Keywords— Adsorption, Cost, Chemical co-precipitation, Magnetic activated carbon, Characterisation, Chemical impregnation

1 INTRODUCTION

Activated carbon (AC) has long been utilised as a formidable adsorbent in wastewater treatment. One of its major setbacks has been the recovery of adsorbent particles in wastewater treatment mix to avoid sludge formation and enable regeneration for reuse. These post treatment challenges have been addressed with the recent advent of magnetically enhanced activated carbons (Yi et al., 2020; Borghi et al., 2013). While AC is widely recognised for its high specific surface area and versatile chemistry (Ahmedna et al., 2000), the separation of spent powdered adsorbents through conventional methods like filtration has been an operational bottleneck that adds complexity and treatment cost (Moosavi et al., 2020). However, magnetisation techniques allow the adsorption capacity of AC to be combined with magnetic properties to achieve separation via an external magnetic field, improving adsorbent recyclability and reduction in formation sludge (Mohan et al., 2011).

Chemical co-precipitation and impregnation methods are among widely used methods magnetisation techniques utilised to produce magnetised activated carbons (MACs) (da Silva et al., 2021). These methods differ in terms of how they achieve synthesise a magnetic material and the changes they bring on the structures of the adsorbent. These mechanistic differences create a critical physicochemical trade-off. Magnetisation often leads to a loss of textural properties due to blockage, but its simultaneously introduces additional surface functionalities that serve as additional adsorption centres (Mohan et al., 2011). As operational conditions of synthesis dictate these properties (Gale et al., 2021), it is essential to systematically evaluate how each method influences performances in adsorption. Despite this, there are limited comparative studies that integrate physicochemical analysis, adsorption modelling, and economic feasibility assessment under identical experimental conditions for different magnetisation synthesis routes. Among the most soluble, toxic, and persistence metal ions in worldwide, chromium (Cr) is reported to widely contaminate surface waters (Nemeș et al., 2026). This makes Cr contaminated wastewater an ideal matrix for evaluating the MACs. Patel (2022) revealed that testing the capacity of adsorbents through batch experiments is fundamental for their characterisation as it provides valuable insight into adsorption mechanisms.

This study provides a comparative evaluation of MACs synthesised through chemical co-precipitation and chemical impregnation. By integrating detailed physicochemical characterisation, adsorption modelling and economic assessment, this work establishes a technical basis for selection and design of cost-effective, magnetically separable adsorbents for heavy metal removal in wastewater treatment.

Corresponding Author:
Section D- MATERIALS & METALLURGICAL/CHEMICAL ENGINEERING & RELATED SCIENCES
Can be cited as:
Musa A., Sani B. S., Abubakar U. A., and Adie D. B. (2026). Comparative Evaluation of Magnetic Activated Carbon Synthesised Using Chemical Co-Precipitation and Impregnation for Heavy Metal Removal. FUOYE Journal of Engineering and Technology (FUOYE**JET), 11(3), 519-524.**
https://dx.doi.org/10.46792/fuoyejet.v11i3.1596

© 2026 The Author(s). Published by Faculty of Engineering, Federal University Oye-Ekiti.
This is an open access article under the CC BY NC license. (https://creativecommons.org/licenses/by-nc/4.0/)

2 METHODOLOGY

2.1 SYNTHESIS OF MAGNETIC ACTIVATED CARBON

For the co-precipitation route, MAC was synthesised in accordance to Han et al. (2015) but slightly modified to scale-up the quantity required. 50 g of AC was dispersed in 2 L of deionised water under continuous stirring. $FeSO_4{\cdot}7H_2O$ (36.6 g) and $FeCl_3{\cdot}6H_2O$ (66.6 g) were added, and the mixture was heated to 65–70 °C. After cooling below 40 ℃, the pH level was brought to 10–11 by adding 0.5 M NaOH dropwise. The mixture was aged overnight before decanting the supernatant and the precipitate collected magnetically, repeatedly rinsed with deionised water and ethanol, then oven-dried at 80 °C for 6 hr. The product was designated chemically precipitated-magnetic activated carbon (CP-MAC).

The chemical impregnated MAC was prepared in accordance to Nguyen et al. (2011) with scale-up. 50 g of AC was mixed in 100 mL solution of containing deionised water (80 mL), 20.2 g of $Fe(NO_3)_3{\cdot}9H_2O$, and 16 M HNO_3 (20 mL). The mixture was aged for 24 hr. The material was then pyrolysed in a tubular furnace (Gallenkamp, UK) at 600 ℃ for 1 hr under a constant N_2 supply. After cooling, the material was collected magnetically and designated chemically impregnated magnetic activated carbon (CI-MAC).

2.2 CHARACTERISATION OF MAGNETIC ACTIVATED CARBON

2.2.1 TEXTURAL PROPERTIES

The specific surface area (SA_{BET}), micropore volume (V_{mic}) of AC, CP-MAC, and CI-MAC were determined by N_2 adsorption-desorption at -196 ℃ (77 K) after outgassing 0.25 g of each sample at 250 ℃ for 3 hr using a Quantachrome NOVA 4200e analyser. The Brunauer-Emmett-Teller (BET) equation (1) was used to estimate the monolayer adsorption capacity (V_m) from which the S_{BET} was calculated using equation (2) in accordance to Ladavos et al., (2012). The micropore volume was calculated using the Dubinin-Radushkevich (D-R) equation (3) (Saeidi et al., (2016).

$$(P/P_0)/[V-(P/P_0)] = 1/CQ_m + (C-1)(P/P_0/CV_m) \quad (1)$$

$$SA_{BET} = 4.356V_m \quad (2)$$

$$\ln V = \ln V_{mic} - B[RT\ln(P_0/P)]^2 \quad (3)$$

Where Q_m is the N_2 monolayer adsorption capacity (cm^3/g), V_{mic} is the micropore volume (cm^3/g), V is the volume of adsorbed gas (cm^3/g), P is the pressure at equilibrium (atm), P_0 is the saturation pressure (atm), C is the BET constant (dimensionless), R is the universal gas constant (J/mol/K), B is the D-R constant (mol^2/J^2).

2.2.2 SURFACE MORPHOLOGY AND ELEMENTAL COMPOSITION

Surface morphology was analysed using a scanning electron microscope integrated with energy-dispersive X-ray spectroscopy (SEM-EDX; Thermo Scientific, Phenom ProX) at 15 kV voltage, 60 Pa chamber pressure, 2000x magnification and 6.690 mm working distance. The EDX system utilised characteristic X-ray emissions to quantify the elemental composition.

2.2.3 SURFACE FUNCTIONAL GROUPS

Fourier Transform Infrared (FTIR) analysis was performed with an Agilent Technologies Cary 630 spectrometer with the spectral window of 650–4000 cm^{-1} at a resolution of 4 cm^{-1}.

2.2.4 POINT OF ZERO CHARGE

The point of zero pH (pH_{PZC}) was determined in accordance to Mohan et al. (2011). A set of 0.1 M NaCl solutions with starting pH levels of 2, 4, 6, 8, and 10 were prepared for the analysis. Exactly 40 mg of samples were added to 20 mL of each solution and agitated for 12 hr. The final pH levels were recorded, and change in pH (ΔpH) was plotted against initial pH values. The point at which ΔpH equalled zero was identified as the point of zero charge (pH_{PZC}).

2.2.5 BULK DENSITY

Bulk density (ρ_b) was determined using tapped procedure in accordance to Oni et al. (2020). Each adsorbent was oven-dried at 80 ℃ for 1 hr. The weight of the adsorbent sample was measured placed into a 10 mL cylinder, then tapped until the level was consistent without dropping. ρ_b was calculated using equation (4).

$$\rho_b = W/V_{sample} \quad (4)$$

Where W is the weight of oven dried adsorbent (g) and V_{sample} is the packed volume (cm^3).

2.2.6 BATCH ADSORPTION EXPERIMENTS

The procedure was adapted from Mohan et al. (2011). Working solutions of 3.21, 7.16, 11.82, 16.99, 23.77, and 32.21 mg/L were obtained by serial dilution from an initial Cr(VI) solution prepared from concentrated $K_2Cr_2O_7$ using deionised water. For each run, 0.10 g of adsorbent was introduced into 50 mL solution of Cr(VI) in 100 mL vials including blank controls without adsorbent. The suspensions were stirred in a shaker at 130 rpm for 5 hr. The suspensions were filtered (Whatman No. 1), and the equilibrium concentrations in the filtrate were quantified using an atomic absorption spectrophotometer (Agilent Technologies, 280FS AA) following calibration ensuring high linearity. The equilibrium adsorption capacity, q_e (mg/g), was calculated using equation (5) (Foo & Hameed, 2010).

$$q_e = (C_0 - C_e)V/m \quad (5)$$

Where C_0 and C_e are the initial and equilibrium concentrations of Cr(VI) (mg/L), V represents the volume of solution (L), and m is the mass of the adsorbent (g).

2.2.7 NONLINEAR ISOTHERM MODELLING

The Langmuir model (Lang) assumes adsorption occurs on uniformly on a surface with fixed number of identical monolayer sites, with no lateral interaction between molecules on neighbouring sites (Foo & Hameed, 2010). Its nonlinear form is expressed in Equation (6) (Foo & Hameed, 2010).

$$q_e = q_m K_L C_e/1 + K_L C_e \quad (6)$$

Where q_m represents the adsorbate maximum monolayer adsorption capacity (mg/g) and K_L is the Langmuir

© 2026 The Author(s). Published by Faculty of Engineering, Federal University Oye-Ekiti.

This is an open access article under the CC BY NC license. (https://creativecommons.org/licenses/by-nc/4.0/)
http://dx.doi.org/10.46792/fuoyejet.v11i3.1596 engineering.fuoye.edu.ng/journal

affinity constant (L/mg). The Freundlich model (Freu) describes adsorption on surfaces with varied characteristics and nonuniform energy distribution and potential multiple layers of adsorbed molecules, and its nonlinear expression is given in equation (7) (Kumar & Sivanesan, 2005).

$$q_e = K_F C_e^{1/n} \quad (7)$$

where K_F (mg/g)(L/mg)$^{1/n}$ represents adsorption capacity and $1/n$ is the heterogeneity factor.

Parameters of the model were determined using nonlinear regression analysis by reducing the total squared differences between observed data and experimental and values predicted the model. The model adequacy was assessed through the use of the coefficient of determination (R^2) and root mean square error (RMSE) metrics as expressed in equations (8) and (9), respectively (Chen, 2015).

$$R^2 = 1 - \left[(q_e)_{exp,i} - (q_e)_{pred,i}\right]^2 / \left[(q_e)_{exp,i} - (\overline{q_e})_{exp,i}\right]^2 \quad (8)$$

$$RMSE = 100\sqrt{1/n - p\sum_{i=1}^{n}\left[(q_e)_{exp,i} - (q_e)_{pred,i}\right]^2} \quad (9)$$

Where $(q_e)_{exp}$ represents the measured maximum adsorption capacity under experimental conditions (mg/g), $(q_e)_{pred}$ is the predicted equilibrium adsorption capacity (mg/g), $(\overline{q_e})_{exp}$ is the mean of experimental concentrations, n is the total number of data points used in the analysis, and p represents the number of parameters incorporated within the model.

3 RESULTS AND DISCUSSION

3.1 TEXTURAL AND SURFACE PROPERTIES

From the Table 1, the pristine AC exhibited a SA_{BET} of 329.32 m²/g and V_{mic} of 0.118 cm³/g, characteristics of well-developed activated carbons where microporosity predominates (Ahmedna et al., 2000).

Table 1. Physicochemical properties of fresh and magnetic adsorbents.

Parameter	AC	CP-MAC	CI-MAC
SA_{BET} (m²/g)	329.32	254.61	293.14
V_{mic} (cm³/g)	0.118	0.090	0.103
ρ_b (g/cm)	0.500	0.601	0.532
pH_{PZC}	8.200	5.300	7.900

Following magnetisation, both synthesis routes experienced a decline in porosity, signifying partial pore filling and structural densification (Han et al., 2015). CP-MAC exhibited a pronounced 22.69% reduction in SA_{BET} and a 23.78% loss in V_{mic}. Similar reductions have been reported by previous studies (Castro et al., 2009; Oliveira et al., 2002). According to Gale et al. (2021), this suggests that alkaline co-precipitation promotes nucleation within internal structures, leading to pore blockage and structural compaction. While CI-MAC demonstrated a greater structural preservation with smaller decline in SA_{BET} (11.0%) and V_{mic} (12.71%). Nguyen et al., (2011) reported that the impregnation-pyrolysis route favoured surface anchoring and controlled dispersion of iron oxide phases, where they observed similar textural changes. This textural decline represents a structural-functional trade-off. While magnetisation reduces physical accessibility, the incorporation of Fe-OH groups introduces high affinity centres, potentially enhancing chemical reactivity over purely textural adsorption (Castro et al., 2009).

The ρ_b increased from 0.500 g/cm (AC) to 0.601 g/cm (CP-MAC) and 0.532 g/cm (CI-MAC). The higher density of CP-MAC suggests superior structural stability and potential for improved hydraulic performance if utilised in packed column operations (Safarik et al., 2018).

The pristine AC exhibited a basic surface (pH_{PZC} = 8.20), CI-MAC retained a near neutral pH_{PZC} (7.90), while CP-MAC shifted significantly to a more acidic pH_{PZC} of 5.30. This shift is attributable to the high loading of Fe-OH functionalities that can act as both acids and bases (Mohan et al., 2011). Hence, at circumneutral wastewater pH, CP-MAC is more likely to have a negative surface charge, enhancing electrostatic attraction for cationic metal species, whereas at $pH < pH_{PZC}$, the positively charged surface would favour the adsorption of oxyanions (Han et al., 2015).

3.2 MORPHOLOGICAL AND ELEMENTAL CHARACTERISTICS

SEM analysis (Fig. 1) revealed that the pristine AC exhibited heterogenous porous network with interconnected cavities, a characteristic morphology of chemically activated carbons that facilitates efficient intraparticle diffusion and active site accessibility (Radovic, 2008).

CI-MAC micrographs reveal finely dispersed iron-containing particles distributed along pore walls without substantial collapse of the carbon framework. The impregnation-pyrolysis route favoured controlled dispersion of iron oxide phases. It limited agglomeration and preserved structural integrity. This aligns with the moderate changes in SA_{BET} and V_{mic} and suggests that CI-MAC remains predominantly carbonaceous, with iron phases acting as discrete functional domains (Nguyen et al., 2011). In contrast, CP-MAC exhibited pronounced surface restructuring, characterised by aggregated iron oxide clusters deposited on the external surfaces and within the pore channels. These observations correlate directly with the substantial reductions in SA_{BET} discussed in Section 3.1.

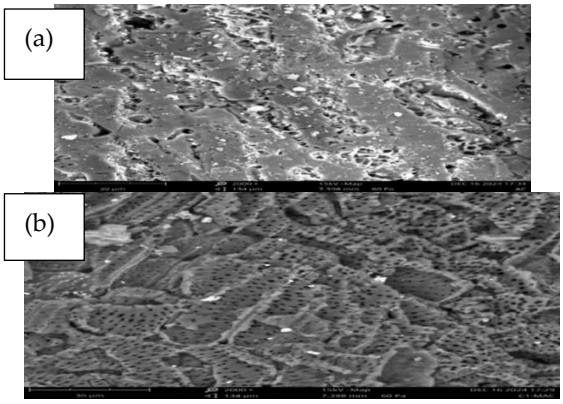

© 2026 The Author(s). Published by Faculty of Engineering, Federal University Oye-Ekiti.
This is an open access article under the CC BY NC license. (https://creativecommons.org/licenses/by-nc/4.0/)

http://dx.doi.org/10.46792/fuoyejet.v11i3.1596 engineering.fuoye.edu.ng/journal

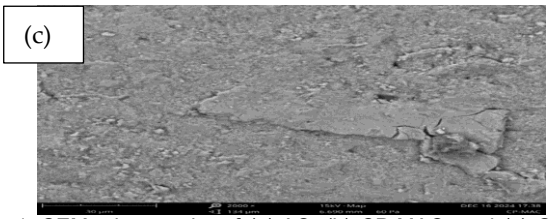

Fig. 1. SEM micrographs of (a) AC, (b) CP-MAC, and (c) CI-MAC captured at 2000x and 30 µm.

Table 2 presents the EDX elemental result (in atomic concentration) while their spectra are shown in Fig. 2 generated spectra. The results show the compositional divergence clearer. Pristine AC was predominantly carbon (75.39% C), reflecting a graphitic-aromatic framework that supports π- π interactions (Radovic, 2008).

Table 2. Elemental composition of the adsorbents.

Samples	AC (%)	CP-MAC (%)	CI-MAC (%)	
Carbon	75.39	2.04	86.98	
Iron	0.00	85.80	1.82	
Nitrogen	9.31	0.00	10.28	
Sulphur	0.08	2.77	0.00	
Chlorine	0.29	1.76	0.14	
Sodium	2.15	5.63	0.00	
Potassium	5.40	0.00	0.78	
Silicon	3.21	0.33	0.00	
Aluminium	2.24	0.85	0.00	
Calcium	1.29	0.00	0.00	
Magnesium	0.65	0.38	0.00	
Phosphorus	0.00	0.13	0.00	
Titanium	0.00	0.12	0.00	
Cobalt	-	0.15	-	
Manganese	0.00	0.18	0.00	

CI-MAC retained high carbon fraction (86.98%) with low iron incorporation (1.82%), indicating that the carbon matrix remained the primary structural component. CP-MAC transitioned into an iron-dominant composite (85.80% Fe) with minimal residual carbon (2.04%).

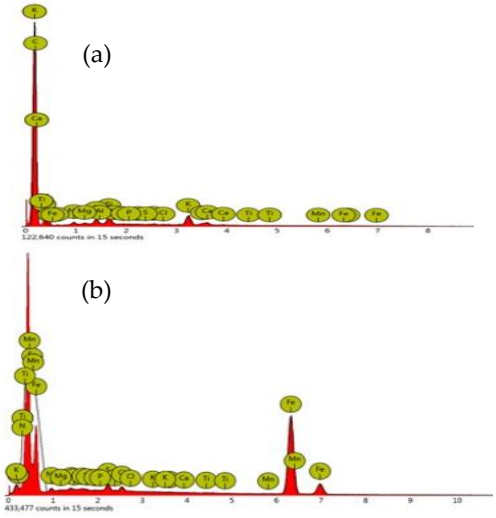

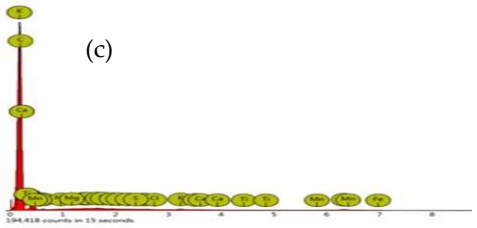

Fig. 2. EDX elemental spectra of (a) AC, (b) CP-MAC, and (c) CI-MAC.

3.3 SURFACE FUNCTIONAL GROUPS

FTIR analysis showed the surface chemical functionality changes that occurred, based on the interaction of the material with infrared light and their measured absorption spectra (Ezinma et al., 2024). Magnetisation induced clear distinctions between impregnation and co-precipitation routes (Fig. 2). The AC exhibited bands at 2653.9 cm^{-1} (O-H stretching), 1688.5 cm^{-1} (C=O stretching of carbonyl/carboxylic groups), and 872.2 cm^{-1} (aromatic C-H vibrations), indicating the presence of oxygen containing functionalities embedded within an aromatic carbon framework. Such surface groups confer amphoteric character and facilitate metal adsorption through electrostatic interactions, hydrogen bonding, and surface complexation (Figueiredo et al., 1999).

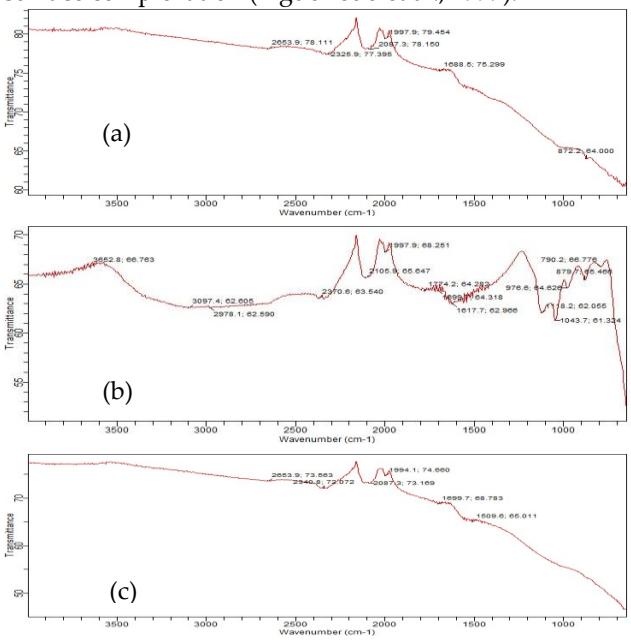

Fig. 3. Comparison of the FTIR spectra of (a) AC (b) CP-MAC and (c) CI-MAC.

CI-MAC largely preserved the carbon-based functional groups. The limited spectral changes suggest that impregnation-pyrolysis process preserved the carbon framework. This aligns with its moderate iron loading and preserved porosity. The persistence of the O-H band (2653.9 cm^{-1}) and the appearance of an aromatic C=C vibrations at 1509.6 cm^{-1} indicate retention of the carbon matrix with limited oxidative disruption. Thus, adsorption is likely to be governed predominantly by carboxylic and phenolic sites, supplemented by dispersed iron oxide domains capable of additional coordination (Li et al., 2002).

© 2026 The Author(s). Published by Faculty of Engineering, Federal University Oye-Ekiti.
This is an open access article under the CC BY NC license. (https://creativecommons.org/licenses/by-nc/4.0/)

http://dx.doi.org/10.46792/fuoyejet.v11i3.1596 engineering.fuoye.edu.ng/journal

In contrast, CP-MAC exhibited extensive chemical restructuring. New bands at 3652.8 cm^{-1} (phenolic O-H), 1774.2 cm^{-1} (anhydride/ester C=O) and 1118.2 and 1043.2 cm^{-1} (alcohol C-O), and prominent Fe-O-H vibrations at 790.2, 879.7, and 976.6 cm^{-1}, confirm extensive formation of Fe-OH which are characteristics of magnetite/goethite structures formed during co-precipitation. Similar bands have been reported by Castro et al., (2009), who noted that the main iron oxide present in the magnetic composites is goethite. They serve as reactive centres for ligand exchange and inner sphere complexation (Yi et al., 2020).

3.4 ADSORPTION ISOTHERM MODELLING

The experimental equilibrium isotherms for the pristine AC and the MACs are presented in figure 3 while Table 2 provides the nonlinear isotherm modelling parameters.

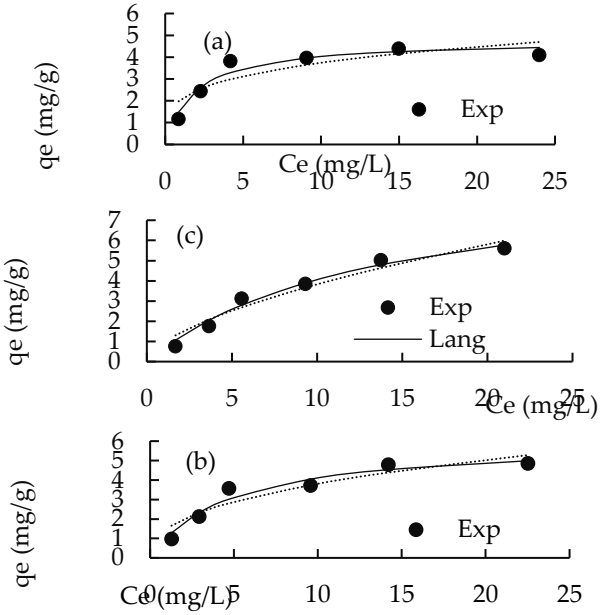

Fig. 4. Experimental vs predicted isotherms for (a) AC (b) CP-MAC and (c) CI-MAC.

CP-MAC demonstrated higher performance, achieving q_e of 5.61 mg/g compared to 4.79 mg/g for CI-MAC. Crucially, CP-MAC outperformed CI-MAC despite having lower SA_{BET} and V_{mic}, indicating that adsorption was not governed by textural accessibility alone (Radovic, 2008) but is also attributed to enriched surface chemistry (Figueiredo et al., 1999).

Table 3. Isotherm model parameters for Cr adsorption obtained using nonlinear regression.

Model	Parameters	AC	CP-MAC	CI-MAC
Lang	q_m	4.80	9.40	6.03
	K_L	0.52	0.08	0.21
	R^2	0.93	0.98	0.95
	RMSE	0.37	0.30	0.40
Freu	K_F	2.06	0.95	1.50
	$1/n$	0.26	0.60	0.40
	R^2	0.76	0.95	0.88
	RMSE	0.68	0.48	0.60

The enhanced chemical surface functionalisation of CP-MAC offers a mechanistic explanation for its superior adsorption capacity despite partial blockage. Similar behaviour has been reported for iron enriched magnetic carbons and biochars, where chemical functionality compensates for moderate porosity loss (Yi et al., 2020). The Langmuir model exhibited superior fit ($R^2 \geq 0.98$; RMSE = 0.30), confirming a site-specific interaction mechanism consistent with monolayer surface complexation. CP-MAC yielded a q_m of 9.40 mg/g and K_L of 0.08 L/mg compared to CI-MAC (q_m = 6.03 mg/g; K_L = 0.21 L/mg). Freundlich analysis corroborated surface heterogeneity, with $1/n$ values for both materials falling within the favourable range ($0 < 1/n < 1$). The higher $1/n$ for CP-MAC further indicates that the adsorption is on a homogeneous surface. According to Li et al. (2002), $1/n$ value closer to one (1.0) depicts a more homogenous adsorbent. The relatively low RMSE and high R^2 values for both CP-MAC and CI-MAC indicate close agreement between experimental and predicted data as presented in Figure 3.

3.5 ECONOMIC EVALUATION OF SYNTHESIS

Cost distributions are primarily governed by a multi-variable trade-off between reagent consumption, energy intensity, labour input, and product yield. While the batch expenditure for CP-MAC (₦8,911.15) exceeded that of CI-MAC (₦6,566.00), the co-precipitation route achieved a higher yield (70 g vs. 45 g). Consequently, the unit production cost for CP-MAC (₦127/g) is lower than that of CI-MAC (₦146/g). This demonstrates that despite higher upfront costs, co-precipitation is more economically efficient on a mass-normalized basis.

The economic differentiating factors between the two routes were labour and energy needs, as raw material expenditures remained relatively comparable (₦4,750 for CP-MAC; ₦4,320 for CI-MAC). The CP-MAC exhibited higher labour intensity, requiring an extensive processing timeframe (7.5 hr; ₦3,281.25) to manage precipitation kinetics and rigorous washing protocols. In contrast, CI-MAC incurred higher energy costs (₦1,152.25 vs. ₦879.90) necessitated by high temperature pyrolysis (5.5 kWh) and the maintenance of an inert gas environment. Given the prevailing electricity tariffs (₦209.50/kWh), energy demand represents a critical constraint. Thus, the lower thermal requirement of CP-MAC offers a distinct strategic advantage in energy constrained settings.

When adsorption performance is considered with these economic metrics, CP-MAC demonstrates superior cost-performance profile, implying that a lower adsorbent mass is required to achieve target Cr(VI) removal levels compared to CI-MAC.

4 CONCLUSIONS

This study demonstrated that magnetisation route critically dictates the physicochemical properties, Cr(IV) removal, and cost viability of MACs. The CP-MAC emerged as the superior adsorbent despite greater textural reductions in SA_{BET} and V_{mic} of 22.69% and 23.78%, respectively. The high iron loading (85.80% Fe) provided the chance for more robust magnetic retrievability and enriched Fe-OH surface functionality. Consequently, CP-MAC achieved a significantly higher Langmuir adsorption capacity (q_m) of 9.40 mg/g compared to 6.03 mg/g for CI-MAC. While CI-MAC

© 2026 The Author(s). Published by Faculty of Engineering, Federal University Oye-Ekiti.
This is an open access article under the CC BY NC license. (https://creativecommons.org/licenses/by-nc/4.0/)

http://dx.doi.org/10.46792/fuoyejet.v11i3.1596 engineering.fuoye.edu.ng/journal

(1.82% Fe) maintained superior structural integrity and porosity, its weaker magnetic response and lower chemical affinity limited its performance. Economic assessment further validated the preference for the co-precipitation route. Production cost for CP-MAC was about 13% lower than that of CI-MAC, representing a cost saving of ₦19/g. These results highlight that CP-MAC offers a higher efficient, magnetically recoverable, and cost-effective adsorbent for Cr(VI) removal from wastewater effluents.

ACKNOWLEDGMENT

The authors acknowledge the technical assistance provided by the staff of the Environmental Chemistry Laboratory, Department of Water Resources and Environmental Engineering, Department of Chemical Engineering, and the Multiuser Research Laboratory, Faculty of Science, Ahmadu Bello University, Zaria, Nigeria.

REFERENCES

Ahmedna, M., Marshall, W. E., & Rao, R. M. (2000). Production of granular activated carbons from select agricultural by-products and evaluation of their physical, chemical and adsorption properties. *Bioresource Technology*, 71(2), 113–123. https://doi.org/10.1016/S0960-8524(99)00070-X

Borghi, C. C., Akiyama, Y., Fabbri, M., Nishijima, S. and Ribani, P. L. (2013). Magnetic separation of magnetic activated carbons for water treatment and reuse. *COMPEL*, 33(1-2), 445-462. https://doi.org/10.1108/COMPEL-03-2013-0088

Castro, C. S., Guerreiro, M. C., Goncalves, M., Oliveira, L. C. A., & Anastácio, A. S. (2009). Activated carbon/iron oxide composites for the removal of atrazine from aqueous medium. *Journal of Hazardous Materials*, 164(2-3), 609–614. https://doi.org/10.1016/j.jhazmat.2008.08.066

Chen, X. (2015). Modeling of experimental adsorption isotherm data. *Information*, 6, 14–22. https://doi.org/10.3390/info6010014

da Silva, T. L., da Costa, T. B., & Neves, H. S. d. C., da Silva, M. G. C., Vieira, M.G.A. (2021). Methods of synthesis of magnetic adsorbents. In Advanced *magnetic adsorbents for water treatment. Environmental chemistry for a sustainable world* (pp. 25–58). Springer, Cham. https://doi.org/10.1007/978-3-030-64092-7_2

Ezinma, E., Nurudeen, S., Sani, A., Ibeh, J., & Nuhu, A. (2024). Isotherm study of methylene blue (Mb) adsorption on activated carbon synthesised from Wheat Straw Biomass. *FUOYE Journal of Engineering and Technology (FUOYEJET)*, 9(4), 669–676. https://doi.org/10.4314/fuoyejet.v9i4.16

Figueiredo, J. L., Pereira, M. F. R., Freitas, M. M. A., & Órfão, J. J. M. (1999). Modification of the surface chemistry of activated carbons. *Carbon*, 37(9), 1379-1389. https://doi.org/10.1016/S0008-6223(98)00333-9

Foo, K. Y., & Hameed, B. H. (2010). Insights into the modeling of adsorption isotherm systems. *Chemical Engineering Journal*, 156(1), 2–10. https://doi.org/10.1016/j.cej.2009.09.013

Gale, M., Nguyen, T., Moreno, M., & Gilliard-AbdulAziz, K. L. (2021). Physicochemical properties of biochar and activated carbon from biomass residue: Influence of process conditions to adsorbent properties. *ACS Omega*, 6(15), 10224–10233. https://doi.org/10.1021/acsomega.1c00530

Han, Z., Sani, B., Mrozik, W., Obst, M., Beckingham, B., Karapanagioti, H. K., & Werner, D. (2015). Magnetite impregnation effects on the sorbent properties of activated carbons and biochars. *Water Research*, 70, 394–403. https://doi.org/10.1016/j.watres.2014.12.016

Kumar, K. V., & Sivanesan, S. (2005). Comparison of linear and non-linear method in estimating the sorption isotherm parameters for safranin onto activated carbon. *Journal of Hazardous Materials*, *123*, 288–292. https://doi.org/10.1016/j.jhazmat.2005.03.040

Ladavos, A. K., Katsoulidis, A. P., Iosifidis, A., Triantafyllidis, K. S., Pinnavaia, T. J., & Pomonis, P. J. (2012). The BET equation, the inflection points of N_2 adsorption isotherms and the estimation of specific surface area of porous solids. *Microporous and Mesoporous Materials*, *151*, 126-133. https://doi.org/10.1016/j.micromeso.2011.11.005

Li, L., Quinlivan, P. A., & Knappe, D. R. U. (2002). Effects of activated carbon surface chemistry and pore structure on the adsorption of organic contaminants from aqueous solution. *Carbon*, 40(12), 2085–2100. https://doi.org/10.1016/S0008-6223%2802%2900069-6

Mohan, D., Sarswat, A., Singh, V. K., Alexandre-Franco, M., & Pittman Jr., C. U. (2011). Development of magnetic activated carbon from almond shells for trinitrophenol removal from water. *Chemical Engineering Journal*, 172(2–3), 1111–1125. https://doi.org/10.1016/j.cej.2011.06.054

Moosavi, S., Lai, C. W., Gan, S., Zamiri, G., Akbarzadeh Pivehzhani, O., & Johan, M. R. (2020). Application of efficient magnetic particles and activated carbon for dye removal from wastewater. *ACS omega*, *5*(33), 20684–20697. https://doi.org/10.1021/acsomega.0c01905

Nemeș, N. S., Negrea, A., Ciopec, M., Negrea, P., Duţeanu, N., & Duda-Seiman, D. M. (2026). Heavy metal ion removal: A global review of wastewater treatment technologies. *International Journal of Molecular Sciences*, *27*(4), 1741. https://doi.org/10.3390/ijms27041741

Nguyen, T. D., Phan, N. H., Do, M. H., & Ngo, K. T. (2011). Magnetic Fe_2MO_4 (M: Fe, Mn) activated carbons: Fabrication, characterization and heterogeneous Fenton oxidation of methyl orange. *Journal of Hazardous Materials*, 185(2–3), 653–661. https://doi.org/10.1016/j.jhazmat.2010.09.068

Oliveira, L. C. A., Rios, R. V. R. A., Fabris, J. D., Garg, V., Sapag, K., & Lago, R. M. (2002). Activated carbon/iron oxide magnetic composites for the adsorption of contaminants in water. *Carbon*, 40(12), 2177–2183. https://doi.org/10.1016/S0008-6223(02)00076-3

Oni, B. A., Abatan, O. G., Busari, A., Odunlami, O., & Nweke, C. (2020). Production and characterization of activated carbon from pineapple waste for treatment of kitchen wastewater. *Desalination and Water Treatment*, *183*, 413–424. https://doi.org/10.5004/dwt.2020.25371

Patel, H. (2022). Comparison of batch and fixed bed column adsorption: a critical review. *International Jornal of Environmental Science and Technology*, 19, 10409–10426. https://doi.org/10.1007/s13762-021-03492-y

Radovic, L. R. (2008). Physicochemical properties of carbon materials: A brief overview. In: Serp, P. & Figueiredo, J.L., *Carbon Materials for Catalysis*. Wiley. pp. 1–44. https://doi.org/10.1002/9780470403709

Saeidi, N., & Parvini, M. (2016). Accuracy of Dubinin-Astakhov and Dubinin-Radushkevich adsorption isotherm models in evaluating micropore volume of bentonite. *Periodica Polytechnica Chemical Engineering*, *60*(2), 123-129. https://doi.org/10.3311/PPch.8374

Safarik, I., Baldikova, E., Prochazkova, J., Safarikova, M., & Pospiskova, K. (2018). Magnetically modified agricultural and food waste: Preparation and application. *Journal of Agricultural and Food Chemistry*, 66(11), 2538–2552. https://doi.org/10.1021/acs.jafc.7b06105

Yi, Y., Huang, Z., Lu, B., Xian, J., Tsang, E. P., Cheng, W., Fang, J. & Fang, Z. (2020). Magnetic biochar for environmental remediation: A review. *Bioresource Technology*, 298, 122468. https://doi.org/10.1016/j.biortech.2019.122468

© 2026 The Author(s). Published by Faculty of Engineering, Federal University Oye-Ekiti.
This is an open access article under the CC BY NC license. (https://creativecommons.org/licenses/by-nc/4.0/)